6-5-2012

Human genome-wide association and mouse knockout approaches identify platelet supervillin as an inhibitor of thrombus formation under shear stress.

Leonard C. Edelstein
Thomas Jefferson University

Elizabeth J. Luna
University of Massachusetts, Worcester

Ian B. Gibson
Baylor College of Medicine

Molly Bray
University of Alabama at Birmingham

Ying Jin
Thomas Jefferson University

See next page for additional authors

Human Genome-Wide Association and Mouse Knockout Approaches Identify Platelet Supervillin as an Inhibitor of Thrombus Formation under Shear Stress

Leonard C. Edelstein PhD[1], Elizabeth J. Luna PhD[2], Ian B. Gibson[3], Molly Bray PhD[4], Ying Jin MD[1], Altaf Kondkar PhD[1], Srikanth Nagalla MD[1], Nacima Hadjout-Rabi PhD[2], Tara C. Smith[2], Daniel Covarrubias PhD[3], Stephen N. Jones PhD[2], Firdos Ahmad PhD[1], Moritz Stolla[1], Xianguo Kong MD[1], Zhiyou Fang PhD[2], Wolfgang Bergmeier PhD[5], Chad Shaw PhD[3], Suzanne M. Leal PhD[3,6], Paul F. Bray MD[1]

1. Thomas Jefferson University, The Cardeza Foundation for Hematologic Research and the Department of Medicine, Jefferson Medical College, Philadelphia, Pennsylvania, USA; 2. Department of Cell Biology, University of Massachusetts, Worcester, MA, USA; 3. Department of Genetics, Baylor College of Medicine, Houston, Texas, USA; 4. Departments of Epidemiology and Genetics, University of Alabama at Birmingham, Birmingham, AL USA; 5. Department of Biochemistry and Biophysics, University of North Carolina, Chapel Hill, NC, USA. 6. Department of Statistics, Rice University, Houston, Texas, USA

Corresponding author: Paul F. Bray, MD, Thomas Jefferson University, The Cardeza Foundation for Hematologic Research and the Department of Medicine, Jefferson Medical College, Curtis Building, Room 324, 1015 Walnut St., Philadelphia, Pennsylvania 19107. Telephone: (215) 955-8544; Fax: (215) 955-9170; E-mail: paul.bray@jefferson.edu

Journal Subject Codes: 145, 89, 146, 172, 92, 178

Word Count: 6995

Abstract

Background

High shear force critically regulates platelet adhesion and thrombus formation during ischemic vascular events. To identify genetic factors that influence platelet thrombus formation under high shear stress, we performed a genome-wide association study (GWAS) and confirmatory experiments in human and animal platelets.

Methods and Results

Closure times in the shear-dependent Platelet Function Analyzer (PFA)-100® were measured on healthy, non-diabetic European Americans (n=125) and African Americans (n=116). A GWAS significant association ($p<5X10^{-8}$) was identified with 2 SNPs within the *SVIL* gene (chr 10p11.23) in African-Americans but not European Americans. Microarray analyses of human platelet RNA demonstrated the presence of *SVIL* isoform 1 (supervillin) but not muscle-specific isoforms 2 and 3 (archvillin, SmAV). *SVIL* mRNA levels were associated with *SVIL* genotypes ($p\leq0.02$) and were inversely correlated with PFA-100 closure times ($p<0.04$) and platelet volume ($p<0.02$). Leukocyte-depleted platelets contained abundant levels of the ~205 kD supervillin polypeptide. To assess functionality, mice lacking platelet supervillin were generated and back-crossed onto a C57BL/6 background. Compared to controls, murine platelets lacking supervillin were larger by flow cytometry and confocal microscopy, and exhibited enhanced platelet thrombus formation under high shear, but not low shear, conditions.

Conclusions

We show for the first time that 1) platelets contain supervillin, 2) platelet thrombus formation in the PFA-100® is associated with human *SVIL* variants and low *SVIL* expression, and 3) murine platelets lacking supervillin exhibit enhanced platelet thrombus formation at high shear stress. These data are consistent with an inhibitory role for supervillin in platelet adhesion and arterial thrombosis.

Key Words: platelets, genetics, thrombosis

Introduction

Arterial thrombosis is a major cause of myocardial infarction (MI) and stroke. Most clinical events occur when an atherosclerotic plaque ruptures to expose subendothelial collagen and von Willebrand factor (VWF). These proteins bind to platelets triggering primary activation and granule secretion.[1] Secretion of soluble agonists, including ADP, amplifies activation and leads to integrin activation, platelet-platelet aggregation and occlusive thrombus formation. Platelets play a more prominent role in arterial thrombus formation than in venous thrombosis because the highly specialized initial platelet-VWF interaction is enhanced by shear stress, such as occurs in coronary arteries.[2, 3]

Platelet reactivity varies greatly among individuals. This variation exhibits strong heritability in both European Americans (EA) and African Americans (AA)[4], which could explain some of the known genetic contribution to the risk of acute MI.[5] Although genetic epidemiology screens have identified loci associated with MI risk[6], our understanding of causative genes is limited. The use of intermediate phenotypes to identify genes involved in the pathophysiology of arterial thrombosis can yield stronger genetic associations.[7] Genome-wide association studies (GWAS) have led to the discovery of key molecules regulating human disease[8] and have identified genetic variants and novel genes associated with platelet number, platelet volume and *in vitro* platelet aggregation.[9, 10] However, no GWAS has identified genes associated with shear stress-dependent platelet function. The Platelet Function Analyzer-100® (PFA-100) measures the time to platelet thrombus formation under a defined shear stress of 1500 sec^{-1} in whole blood.[11] The assay requires platelet tethering to VWF, firm adhesion to collagen, platelet activation and secretion, and platelet aggregation mediated by VWF and fibrinogen. Abnormal assay results correlate with platelet hyperfunction and hypofunction associated with acute coronary syndromes[12-15] and bleeding disorders, respectively.[16, 17] The aim of this study was to identify genetic factors that influence platelet reactivity and thrombus formation under high shear

stress. We carried out a genome-wide screen with the PFA-100® to identify novel gene variants in AAs and EAs. We identified a novel platelet gene, *SVIL* (encoding the cytoskeletal regulatory protein, supervillin), whose expression negatively regulates platelet reactivity and thrombus formation in both humans and mice.

Methods

Subjects and platelet phenotyping. The Platelet Genes and Physiology study was approved by the Institutional Review Boards of Baylor College of Medicine and Thomas Jefferson University, and informed consent was obtained from all volunteers. Healthy donors were recruited between 2000-2006 in Houston, Texas. Citrated whole blood was used to measure PFA-100® closure times in a collagen and ADP-impregnated cartridge (hereafter referred to as PFA-100ColA) within 30 min of phlebotomy. A platelet aggregation response of <10% was considered as exposure to anti-platelet agents and reason for exclusion.

Genotyping. Genomic DNA was extracted from leukocyte buffy coats with the Qiagen DNA extraction kit (Qiagen, Valencia, CA, USA) according to the manufacturer's instructions. DNA from AAs was genotyped on the Illumina Hum1M Beadarray. EA DNAs were genotyped on the Illumina Hum550k Beadarray. Due to the lower levels of linkage disequilibrium (LD) in African populations a denser SNP micorarray was selected to genotype the DNA samples from AA individuals to improve tagging of causal variants.

Statistical analysis. Quality control was performed before statistical analysis. Subjects were excluded for relatedness to other participants and for failing stringent genotyping quality control. Individual genotypes that failed quality control were also removed (see Supplemental Methods for details). PFA-100ColA closure times were natural log transformed and tested for associations using an additive model within a linear regression framework. All analyses of EA and AA samples were performed separately. The potential confounders, age, sex, VWF activity, plasma fibrinogen level and platelet CD41 level were tested for significance using forward selection and significant covariates were retained within the model (p-value < 0.1). Principal Components Analysis (PCA) was also performed on the data using a subset of the SNP markers that are in linkage equilibrium (r^2<0.3).[18] To evaluate if there is inflation of the test statistic due to population substructure/admixture, lambda, was estimated when both no PCA components and when one through five PCA components were included in the linear regression

model. For those SNPs that met GWAS significance (p-value < 5 X10-8) a dominance parameter was tested in a linear regression model in order to determine whether the data fit an additive model where the genetic effect for the heterozygous genotype is between that of the genetic effects for the two homozygous genotypes for the major, reference allele, and the minor allele.

Platelet gene expression analysis. RNA from leukocyte-depleted platelets (LDP) was prepared for gene expression profiling in 29 healthy subjects. LDP was prepared using density centrifugation followed by CD45-positive cell depletion of platelet rich plasma (PRP).[19] As controls, RNA from PRP and from the CD45+ leukocyte fraction was extracted from 11 and 5 subjects, respectively, using TRIzol® (Invitrogen, Carlsbad, CA). Gene expression analysis was performed using the Sentrix BeadChip and BeadStation system from Illumina, Inc. (San Diego, CA).[20]

Platelet supervillin expression and correlation with PFA-100ColA. LDP RNA was used to validate the *SVIL* microarray data.[19] Total LDP RNA was reverse transcribed and PCR-amplified using a sense primer in exon 1 and an antisense primer in exon 5. Immunoblotting of 6% SDS-PAGE gels was performed with 4 different anti-supervillin antibodies to verify platelet expression. Natural log transformed mRNA expression data from microarrays was plotted *vs.* PFA-100ColA closure times for the 23 individuals for whom both values were available. Pearson correlation r- and P-values were calculated using GraphPad Prism software (La Jolla, CA).

Mouse platelet phenotyping. Mice lacking Svil were generated and back-crossed ten times onto a C57BL/6 background. *Svil-/-* and control C57BL/6 mice were maintained by homozygous breeding. Platelet thrombus formation under shear stress was measured using microfluidic flow chambers with immobilized collagen.[21] Blood from 3 wild type and 3 *Svil* -/- mice was studied. Experiments were performed over 4 different days, with 3-4 runs per day (a "run" defined as data acquisition from platelet deposition in a single flow chamber) for a total of

15 runs per wild type and 15 runs per *Svil* -/- genotypes. P values were computed using a two-way repeated measures, linear mixed effects ANOVA model that accounts for the main effect of genotype with GraphPad Prism.

Flow Cytometry. Whole blood was diluted into Tyrode's buffer containing 1 mM $CaCl_2$, and stained with FITC-α-CD41 (BD Pharmingen) or PE-α-GPIbα (Emfret Analytics, Würzburg, Germany). After dilution with PBS the cells were analyzed on a FACScan.

Immunofluorescence confocal microscopy. Platelets adhered to glass slides statically, or to collagen coated coverslips statically or under high shear were stained with Alexa-568 phalloidin and α-myosin IIA antibodies and imaged using confocal microscopy.

Additional details are available in the Supplemental Methods.

Results

SNPs within SVIL are associated with platelet function under shear stress

To assess the capacity for platelet thrombus formation under shear stress, PFA-100ColA was used to measure PFA-100® closure times in a cohort of healthy, non-diabetic subjects (the Platelet Genes and Physiology [PGAP] study). For this genetic study, only subjects self-identified as EA or AA were considered. Blood was collected for PFA-100ColA testing on 154 AAs and 157 EAs. The PFA-100ColA closure time data were normally distributed in both groups (not shown). The DNA from each subject was genotyped for 620,901 or 1,070,000 tagSNPs for EAs or AAs, respectively, using the Infinium II platform. Exclusion criteria included NSAID use, subject relatedness and failing genotyping quality control (described in the Methods and in the Supplemental Materials). Table 1 summarizes the demographics of the 116 AA and 125 EA subjects who were analyzed.

The PFA-100ColA phenotype was tested for association with each genotype under an additive model. Using log-transformed values of the PFA-100ColA phenotype, analysis was performed using linear regression, controlling for sex, age, CD41 and VWF activity in AAs, and sex and VWF activity in EAs. For AAs, age ($p=\sim10^{-2}$), sex ($p=\sim10^{-2}$), CD41 ($p=\sim10^{-2}$) and VWF activity ($p=\sim10^{-9}$) were significant and were retained in the model. For EAs, only sex ($p=\sim10^{-2}$) and VWF activity ($p=\sim10^{-9}$) were significant, so only these covariates were included in the analysis. PCA components were not included in the analysis, because lambda=1.0 indicating no inflation in the test statistic due to population substructure/admixture. Figure 1A shows Manhattan plots for genotype associations with PFA-100ColA closure times, with a prominent "peak" observed in chromosome 10 for AAs. Table 2 lists the SNPs with the 12 lowest P values for AAs. Notably, 5 of these SNPs were clustered within ~21.8 kb of 4 exons within the *SVIL* gene, which encodes differentially spliced isoforms of supervillin and archvillin. The most significant SNP, rs7070678 ($p=3.6 \times 10^{-8}$), which is a synonymous SNP in exon 14 of the *SVIL*

gene, is in LD with other SNPs within the *SVIL* gene but not with SNPs in neighboring genes (Figure 1B). A second SNP, rs10826650, within the *SVIL* gene (intron 13) also reached GWAS significance ($p<5X10^{-8}$). Three additional SNPs (rs7910521, rs10826649, rs7913801) within introns 16 and 17 of the *SVIL* gene had p-values in the order of 10^{-6}. To determine whether or not an additive model best fit the data for the SNPs within the *SVIL* gene, a dominance parameter was included in the analysis. However, because the dominance parameter was not significant, it was not included in the model. This parameter was not significant, indicating no more explanatory power was derived from a dominant model. The closest other well-annotated genes in this region, *LYZL1* (lysozyme-like 1) and *KIAA1462*, were >214 kb from the *SVIL* SNPs listed in Table 2, and there was no evidence of an association with either of these genes. The clustering of SNPs with p values of ~10^{-8} suggested that genetic variants in *SVIL* (and not another gene) are associated with PFA-100ColA closure times in AAs. No associations with GWAS significance were detected with SNP marker loci within the *SVIL* gene within EA, although 3 additional SVIL SNPs had weak associations in EA ($p<10^{-2}$).

Supervillin mRNA and protein are present in human and mouse platelets

Figure 2 illustrates the *SVIL* exon structure, the two major known mRNAs and the location of rs7070678, the SNP with the strongest association with PFA-100ColA closure times. *SVIL* encodes supervillin, which has a broad cell distribution, and 2 archvillin isoforms, which are enriched in muscle.[22-24] Supervillin forms a high-affinity link between the actin cytoskeleton and the plasma membrane[22] but has not been described in platelets. Because integrin function and rearrangements of the actin cytoskeleton are a crucial aspect of the platelet adhesive process[25], we therefore sought to characterize supervillin in platelets.

Platelet RNA expression analysis was performed with LDP RNA samples from 29 healthy subjects. Probes from the 5'-most and 3'-most exons (Figure 2A) were readily

detectable. However, an RNA signal was not detected for probe ILMN_1659306, which is specific for archvillin and SmAV. Platelet *SVIL* transcripts are expressed at moderately high levels, and are higher than PECAM-1 but lower than GPIbα mRNAs (supplemental Figure 1). Supervillin transcripts were easily detected in LDP RNA by RT-PCR (Figure 2B), validating the microarray data. Figure 2C shows *SVIL* mRNA levels for LDP, PRP and CD45+ leukocytes (WBC) as box plots.

Western immunoblotting identified supervillin at ~205 kDa in PRP (Figure 3A). This polypeptide migrated slightly faster than that seen in control A549 cells, so additional antisera was used to confirm platelet supervillin Mr and immunoreactivity. The locations of the epitopes recognized by these antibodies are shown in Figure 3B. In addition, because supervillin is present in leukocytes,[26, 27] we also analyzed LDP and leukocyte-enriched buffy coat. Using two other antibodies, 205 kDa supervillin was again detected in platelets, as well as in the megakaryocyte cell line, Meg-01, but was not detected in CD45-enriched leukocytes or K562 erythroleukemia cells (Figure 3C, 3D). Finally, supervillin was present in mouse platelets (Figure 3E). Sequencing of platelet *SVIL* mRNA RT-PCR products revealed the same splice form as is present in HeLa cells (not shown).

Supervillin mRNA levels correlate with platelet function under shear, platelet size and with the rs7070678 genotype

Because platelet protein was available from only a few of the 29 subjects used in the platelet RNA expression analysis, we used *SVIL* mRNA levels to test for a correlation with platelet function. Figure 4A shows that *SVIL* mRNA levels correlate with PFA-100ColA closure times ($p = 0.038$). Since longer closure times indicate reduced platelet function, these data suggest *SVIL* expression may inhibit human platelet thrombus formation under shear stress. A trend was observed for a similar relationship between *SVIL* mRNA expression and collagen-

induced platelet aggregation (p = 0.07), but not with ADP-induced platelet aggregation (p = 0.23; data not shown). *SVIL* mRNA levels also correlated negatively with human mean platelet volume (p = 0.016) (Figure 4B). Because both *SVIL* SNPs and *SVIL* transcripts were associated with PFA-100ColA closure times (Figures 1 and 4), we tested whether *SVIL* SNPs were associated with *SVIL* mRNA levels using a recessive model analysis. Figure 4C shows that *SVIL* expression differed significantly by rs7070678 genotype.

Platelets from Svil deficient mice form thrombi faster under shear in flow chamber studies

To further address the role of supervillin in platelet function, we generated mice from BayGenomics ES cells bearing an insertion in the supervillin (Svil) gene (Figure 5). In this mouse, a β-galactosidase/neomycin phosphotransferase (β-gal/neo) gene trap inserted into the large intron downstream of the 13th of the 34 coding exons (Figure 5A) disrupts expression of all characterized Svil splice-forms (not shown).[22-24] The location of the insertion was verified by Southern blotting, which showed that a Bgl II restriction site from the pGT0lxf vector reduced the 11.5-kb Bgl II fragment including coding exon 13 to 7.2 kb (not shown), and by PCR (Figure 5B) with primers specific for either the wild-type (WT) or mutated (Mut) locus (Figure 5A, arrows). This insertion destabilizes the message or protein because supervillin is effectively absent from murine Svil -/- platelets (Figure 5C) and leukocytes (not shown).

To assess the role of supervillin in platelet thrombus formation under shear stress, we analyzed wild-type and Svil-/- platelets in microfluidic flow chamber assays on immobilized collagen.[21] No difference was observed under the “venous” flow rate of 400 sec^{-1} (Figure 6A-6B), but *Svil* -/- platelets showed greater deposition (P<0.05) under arterial flow rates of 1200 sec-1 (Figure 6C-E). Both percent coverage of the collagen-coated area, indicating platelet adhesion to collagen, and sum intensity, indicating thrombus formation, were affected.

Although there was no difference between wild-type and *Svil*-/- mice in platelet numbers, *Svil*-/- platelets appeared to be larger as measured by both forward scatter in flow cytometry and confocal microscopy (Table 3), consistent with the relationship in humans (Figure 4B). However, these larger platelets did not express correspondingly greater levels of major surface adhesion receptors, integrin αIIb or glycoprotein Ibα (Table 3).

Supervillin directly binds F-actin, myosin II heavy chain, filamin, and many other cytoskeletal proteins.[28-31] To better elucidate the cytoskeletal and structural differences between wild-type and *Svil-/-* platelets, we analyzed F-actin and myosin IIA organization using immunofluorescence confocal microscopy. Although these platelet cytoskeletons are similar in appearance when statically adhered to glass (Figure 7A-B vs 7C-D), Svil-/- platelets are more highly spread after activation under high shear flow across collagen (Figure 7E-F vs 7G-H). The intensity of F-actin staining increases after activation of both types of platelets, as expected given the associated polymerization of actin.[32, 33]

Discussion

Inter-individual variation in platelet reactivity contributes to common arterial thrombotic disorders in humans, but there is only a limited understanding of the responsible molecular mechanisms. We screened a cohort of healthy human subjects by genome-wide genotyping for associations with platelet function assessed under shear stress, and identified a candidate gene in AA that was validated using gene expression and platelet physiology approaches. Our major findings were that 1) genetic variants in *SVIL* were associated with closure times in the PFA-100ColA, 2) platelets contain supervillin and little or no archvillin or SmAV, and 3) low or absent platelet supervillin is associated with enhanced thrombus formation under high shear and increased platelet size in both humans and mice.

Growing evidence supports a role for supervillin as a regulator of cytoskeletal-membrane interactions. Among other functions, supervillin increases myosin II contractility, reduces integrin-mediated cell adhesion, and promotes rapid integrin recycling.[34-36] Our data support an inhibitory role for supervillin in regulating the rapid activation and spreading of platelets during thrombus formation on collagen under shear stress, an important determinant of platelet responsiveness in arterial thrombosis. These results are consistent with supervillin inhibition of spreading and integrin function in other cell types.[44-45]

Genome wide associations study. The PFA-100® is dependent upon shear stress and is relatively "high-throughput." We appreciate that some[12-15], but not all[37, 38], clinical cardiovascular outcome studies have observed associations with PFA-100 results. The lack of an association between PFA-100 results and clinical outcomes may be due to some non-physiological conditions, such as anticoagulated blood or an absence of vessel wall. It would be ideal to replicate our findings with other assays in humans, however neither light transmission aggregometry nor impedance aggregometry are performed under conditions considered to apply shear stress to platelets. Our strategy was to use the GWAS as a screen for identifying

novel genes associated with shear-dependent platelet reactivity. However, our study differs from prior platelet genomics studies in that our validation approach employed mRNA expression and physiology experiments. Our statistical analysis was strengthened by the ability to adjust for confounders known to affect platelet adhesion (VWF activity) and aggregation (CD41 levels), which were also shown to be significant in the analysis. Two SNPs in *SVIL* met the threshold for genome-wide significance in AA, and 3 additional *SVIL* SNPs associated with PFA-100ColA closure times with p values of 10^{-6}.

The reason for our inability to detect a similarly strong association in EA is unclear, but probably relates to limited power of a small sample size by typical GWAS standards and the fact that minor allele frequencies were ~20% lower in EAs. Thus, much larger sample sizes might be necessary to detect an association in EAs. Indeed, supplemental data in the genomic analysis by Johnson et al. show modest associations (~10^{-5}) between SNPs in *SVIL* and *in vitro* platelet aggregation in both AAs and EAs [9].

None of the 5 *SVIL* SNPs associated with PFA-100ColA closure times were predicted to affect the protein coding sequence, so we had no reason to suspect that any of these SNPs directly altered supervillin function. This is not unusual since GWAS uses indirect association mapping with tagSNPs that are in LD with causal variants[8]. However, despite a small sample size comprised of both EA and AA in our RNA expression study, eQTL analysis supported an association between these SNPs and *SVIL* mRNA levels (Figure 4C). Thus, at least one genetic mechanism by which *SVIL* variants may regulate platelet reactivity is by altering *SVIL* expression, perhaps via effects on transcription or mRNA stability.

SVIL expression in platelets. *SVIL* mRNA was detected in platelets using a 3'UTR probe that recognizes all *SVIL* transcripts and a 5'UTR probe specific for nonmuscle supervillin (Figure 2). Archvillin mRNAs were not detected in our microarray expression study, consistent with prior data indicating that archvillin and SmAV are mainly expressed in muscle [23]. In addition to the RNA data, immunoblotting with multiple antibodies demonstrated the presence of abundant

supervillin protein in platelets. Using microarray analysis, Watkins et al. reported that *SVIL* mRNA is expressed in multiple hematopoietic cell types including $CD4^+$ and $CD8^+$ T-cells, $CD14^+$ monocytes , $CD19^+$ B-cells, $CD56^+$ natural killer cells, and $CD66b^+$ granulocytes [27]. We also observed *SVIL* mRNA in $CD45^+$ cells (Figure 2C), found supervillin protein in murine thymocytes, splenocytes, macrophages, and neutrophils by immunoblotting (unpublished data), and recovered Coomassie blue-staining amounts of supervillin from bovine neutrophils [26]. While high levels of proteases may have caused degradation in human leukocyte lysates (Figure 3), supervillin is clearly expressed at moderately high levels in platelets (Figures 2C and 3, Suppl. Fig. 1). And since PRP has some contamination with WBCs, our gene expression data suggest that *SVIL* mRNA is expressed at higher levels in platelets than WBCs (Fig. 2C). The basis for the reproducibly faster migration of platelet supervillin, as compared with HeLa and A549 cell supervillin (Figure 3), is unclear because the predicted mRNAs are identical. A likely explanation is a cell type-specific difference in post-translational modifications.

Supervillin and platelet size. Supervillin expression levels are inversely correlated with platelet size in both humans and mice. Although *Svil*-/- platelets are larger, they do not have greater surface expression of several critical adhesive glycoproteins (GPIbα or integrin α_{IIb}), suggesting a possible membrane cytoskeletal defect, rather than premature release of larger platelets from megakaryocytes. There are several possible mechanisms by which supervillin might regulate platelet size. Filamin anchors the GPIb-IX-V complex to the platelet cytoskeleton and binds to supervillin [31, 39]; an altered filamin-GPIbα interaction could produce larger platelets, such as those characteristic of inherited mutations in the gene encoding GPIbα [40, 41]. Other possible mechanisms include altered myosin II function similar to the *MYH9*-associated macrothrombocytopenias [42], or a simple disruption of the actin cytoskeleton that maintains normal platelet size, as in the Wiskott-Aldrich syndrome [43]. The increased platelet size may enhance thrombus formation since high platelet volumes have been associated with MI [16].

Supervillin and platelet function. Supervillin effects on platelet function are most prominent under shear stress. Healthy human subjects expressing higher levels of *SVIL* mRNA exhibit slower platelet thrombus formation in the PFA-100ColA. Platelets in blood from supervillin-deficient mice form thrombi faster under high shear rates in flow chamber studies than is observed for platelets with wild-type Svil (Figure 6). Although the effect of supervillin on platelet adhesion is not dramatic, it is difficult to demonstrate gain-of-function effects, and the increased adhesion observed in Svil null platelets is well in line with other mouse mutants of signaling molecules that limit platelet activation.[44, 45] The mice used in these studies have *Svil* defects in all tissues, and we cannot exclude an indirect effect on platelets. However, the *SVIL* association studies used here and by Johnson et al. [9] utilized an *in vitro* platelet assay consisting only of platelets and plasma (i.e., aggregometry). Taken together, our results strongly suggest an inhibitory role for supervillin in platelet function. .

An inhibitory effect during spreading is consistent with the larger surface profiles observed for supervillin-deficient platelets on collagen after 2 min of flow under high shear (Figure 7). The direction of this effect is consistent with a number of mechanisms. First, the larger initial volumes of unactivated Svil-/- platelets (Table 3) may contribute to their larger surface areas after activation. Second, the loss of supervillin could increase the rate of cell spreading by increasing integrin adhesion to the substrate, or by decreasing myosin II-mediated slowing of the cell spreading rate, as observed in other cell types [34, 35]. Finally, decreased integrity of the membrane-cytoskeleton connection could increase the apparent cross-sectional surface area if Svil-/- platelets are more sensitive to cortical disruption by high shear forces. Further studies are needed to determine which supervillin interactions regulate the early phases of platelet activation and adhesion under high-shear forces.

There are potential clinical implications to our findings. If confirmed in additional studies, these data suggest that *SVIL* variants may contribute to predisposition to cardiovascular disease in AA. Targeting supervillin in a manner that would enhance its activity might have anti-

thrombotic benefit for arterial vascular disease like MI and stroke, a benefit that may be more pronounced in African Americans. Conversely, drugs that interrupt supervillin function in platelets could have untoward effects of promoting thrombosis. Lastly, SNPs in strong LD with the causative SVIL variant may be useful as a biomarker for risk of thrombosis or hemorrhage.

Summary. Combined genome-wide technologies in a cohort with well-characterized platelet function have led to the identification of a novel protein in platelet biology. We have identified a candidate gene meeting GWAS significance, and both human and mouse studies support an inhibitory effect of supervillin in platelet thrombus formation under shear stress. Although the causative variant in *SVIL* has not been identified, these data indicate that genetic variations in *SVIL* expression contribute to variations in human platelet reactivity and support a role for supervillin in arterial thrombosis. Further analysis of *SVIL* variants may lead to a better understanding of the genetic basis for susceptibility to arterial thrombosis.

Acknowledgments

The authors wish to thank Jing-fei Dong for supervising platelet phenotype acquisition and helpful discussions, Angela Bergeron, Carol Sun, Lucia Stefanini and Lin Ma for technical support, and Debra Newman for generously providing PECAM-1 peptides. We thank Dr. Paul Furcinitti (University of Massachusetts Medical School Biomedical Imaging Facility) for assistance in acquiring confocal images.

Funding Sources

This work was supported by National Institutes of Health grants HL88458 (PFB), GM-033048 (EJL), HL094594 (WB) and by Muscular Dystrophy Association grant #3160 (EJL).

Disclosures

The authors have nothing to disclose.

References

1. Ruggeri ZM. Platelets in atherothrombosis. *Nature Medicine*. 2002;8:1227-1234
2. Fredrickson BJ, Dong JF, McIntire LV, López JA. Shear-dependent rolling on von willebrand factor of mammalian cells expressing the platelet glycoprotein ib-ix-v complex. *Blood*. 1998;92:3684-3693
3. Nesbitt WS, Westein E, Tovar-Lopez FJ, Tolouei E, Mitchell A, Fu J, Carberry J, Fouras A, Jackson SP. A shear gradient-dependent platelet aggregation mechanism drives thrombus formation. *Nat Med*. 2009;15:665-673
4. Bray PF, Mathias RA, Faraday N, Yanek LR, Fallin MD, Herrera-Galeano JE, Wilson AF, Becker LC, Becker DM. Heritability of platelet function in families with premature coronary artery disease. *J.Thromb.Haemost.* 2007;5:1617-1623
5. Marenberg ME, Risch N, Berkman LF, Floderus B, de Faire U. Genetic susceptibility to death from coronary heart disease in a study of twins. *New England Journal of Medicine*. 1994;330:1041-1046
6. Ouwehand WH. The discovery of genes implicated in myocardial infarction. *J Thromb Haemost*. 2009;7 Suppl 1:305-307
7. Li W, Wang M, Irigoyen P, Gregersen PK. Inferring causal relationships among intermediate phenotypes and biomarkers: A case study of rheumatoid arthritis. *Bioinformatics.* 2006
8. Manolio TA, Brooks LD, Collins FS. A hapmap harvest of insights into the genetics of common disease. *J Clin Invest*. 2008;118:1590-1605
9. Johnson AD, Yanek LR, Chen MH, Faraday N, Larson MG, Tofler G, Lin SJ, Kraja AT, Province MA, Yang Q, Becker DM, O'Donnell CJ, Becker LC. Genome-wide meta-analyses identifies seven loci associated with platelet aggregation in response to agonists. *Nature Genetics*. 2010;42:608-613
10. Soranzo N, Rendon A, Gieger C, Jones CI, Watkins NA, Menzel S, Doring A, Stephens J, Prokisch H, Erber W, Potter SC, Bray SL, Burns P, Jolley J, Falchi M, Kuhnel B, Erdmann J, Schunkert H, Samani NJ, Illig T, Garner SF, Rankin A, Meisinger C, Bradley JR, Thein SL, Goodall AH, Spector TD, Deloukas P, Ouwehand WH. A novel variant on chromosome 7q22.3 associated with mean platelet volume, counts, and function. *Blood*. 2009;113:3831-3837
11. Kundu SK, Heilmann EJ, Sio R, Garcia C, Davidson RM, Ostgaard RA. Description of an in vitro platelet function analyzer--pfa-100. *Semin.Thromb Hemost.* 1995;21:106-112
12. Ziegler S, Maca T, Alt E, Speiser W, Schneider B, Minar E. Monitoring of antiplatelet therapy with the pfa-100(r) in peripheral angioplasty patients. *Platelets.* 2002;13:493-497
13. Frossard M, Fuchs I, Leitner JM, Hsieh K, Vlcek M, Losert H, Domanovits H, Schreiber W, Laggner AN, Jilma B. Platelet function predicts myocardial damage in patients with acute myocardial infarction. *Circulation*. 2004;110:1392-1397
14. Gianetti J, Parri MS, Sbrana S, Paoli F, Maffei S, Paradossi U, Berti S, Clerico A, Biagini A. Platelet activation predicts recurrent ischemic events after percutaneous coronary angioplasty: A 6 months prospective study. *Thrombosis Research*. 2006;118:487-493
15. Fuchs I, Frossard M, Spiel A, Riedmuller E, Laggner AN, Jilma B. Platelet function in patients with acute coronary syndrome (acs) predicts recurrent acs. *J.Thromb.Haemost.* 2006;4:2547-2552
16. Bray PF. Platelet hyperreactivity: Predictive and intrinsic properties. *Hematology/Oncology Clinics of North America*. 2007;21:633-645
17. Favaloro EJ. Clinical application of the pfa-100. *Curr Opin Hematol*. 2002;9:407-415
18. Price AL, Patterson NJ, Plenge RM, Weinblatt ME, Shadick NA, Reich D. Principal components analysis corrects for stratification in genome-wide association studies. *Nat Genet*. 2006;38:904-909

19. Nagalla S, Shaw C, Kong X, Kondkar AA, Edelstein LC, Ma L, Chen J, McKnight GS, Lopez JA, Yang L, Jin Y, Bray MS, Leal SM, Dong JF, Bray PF. Platelet microrna-mrna coexpression profiles correlate with platelet reactivity. *Blood*. 2011;117:5189-5197
20. Kondkar AA, Bray MS, Leal SM, Nagalla S, Liu DJ, Jin Y, Dong JF, Ren Q, Whiteheart SW, Shaw C, Bray PF. Vamp8/endobrevin is overexpressed in hyperreactive human platelets: Suggested role for platelet microrna. *J.Thromb.Haemost.* 2010;8:369-378
21. Stolla M, Stefanini L, Roden RC, Chavez M, Hirsch J, Greene T, Ouellette TD, Maloney SF, Diamond SL, Poncz M, Woulfe DS, Bergmeier W. The kinetics of alphaiibbeta3 activation determines the size and stability of thrombi in mice: Implications for antiplatelet therapy. *Blood*. 2011;117:1005-1013
22. Pestonjamasp KN, Pope RK, Wulfkuhle JD, Luna EJ. Supervillin (p205): A novel membrane-associated, f-actin-binding protein in the villin/gelsolin superfamily. *J Cell Biol*. 1997;139:1255-1269
23. Oh SW, Pope RK, Smith KP, Crowley JL, Nebl T, Lawrence JB, Luna EJ. Archvillin, a muscle-specific isoform of supervillin, is an early expressed component of the costameric membrane skeleton. *J Cell Sci*. 2003;116:2261-2275
24. Gangopadhyay SS, Takizawa N, Gallant C, Barber AL, Je HD, Smith TC, Luna EJ, Morgan KG. Smooth muscle archvillin: A novel regulator of signaling and contractility in vascular smooth muscle. *J Cell Sci*. 2004;117:5043-5057
25. Nuyttens BP, Thijs T, Deckmyn H, Broos K. Platelet adhesion to collagen. *Thromb Res*. 2011;127 Suppl 2:S26-29
26. Nebl T, Pestonjamasp KN, Leszyk JD, Crowley JL, Oh SW, Luna EJ. Proteomic analysis of a detergent-resistant membrane skeleton from neutrophil plasma membranes. *J Biol Chem*. 2002;277:43399-43409
27. Watkins NA, Gusnanto A, de Bono B, De S, Miranda-Saavedra D, Hardie DL, Angenent WG, Attwood AP, Ellis PD, Erber W, Foad NS, Garner SF, Isacke CM, Jolley J, Koch K, Macaulay IC, Morley SL, Rendon A, Rice KM, Taylor N, Thijssen-Timmer DC, Tijssen MR, van der Schoot CE, Wernisch L, Winzer T, Dudbridge F, Buckley CD, Langford CF, Teichmann S, Gottgens B, Ouwehand WH. A haematlas: Characterizing gene expression in differentiated human blood cells. *Blood*. 2009;113:e1-9
28. Chen Y, Takizawa N, Crowley JL, Oh SW, Gatto CL, Kambara T, Sato O, Li XD, Ikebe M, Luna EJ. F-actin and myosin ii binding domains in supervillin. *J Biol Chem*. 2003;278:46094-46106
29. Wulfkuhle JD, Donina IE, Stark NH, Pope RK, Pestonjamasp KN, Niswonger ML, Luna EJ. Domain analysis of supervillin, an f-actin bundling plasma membrane protein with functional nuclear localization signals. *J Cell Sci*. 1999;112 (Pt 13):2125-2136
30. Crowley JL, Smith TC, Fang Z, Takizawa N, Luna EJ. Supervillin reorganizes the actin cytoskeleton and increases invadopodial efficiency. *Mol Biol Cell*. 2009;20:948-962
31. Smith TC, Fang Z, Luna EJ. Novel interactors and a role for supervillin in early cytokinesis. *Cytoskeleton (Hoboken)*. 2010;67:346-364
32. Jennings LK, Fox JE, Edwards HH, Phillips DR. Changes in the cytoskeletal structure of human platelets following thrombin activation. *J Biol Chem*. 1981;256:6927-6932
33. Loftus JC, Choate J, Albrecht RM. Platelet activation and cytoskeletal reorganization: High voltage electron microscopic examination of intact and triton-extracted whole mounts. *J Cell Biol*. 1984;98:2019-2025
34. Takizawa N, Ikebe R, Ikebe M, Luna EJ. Supervillin slows cell spreading by facilitating myosin ii activation at the cell periphery. *J Cell Sci*. 2007;120:3792-3803
35. Takizawa N, Smith TC, Nebl T, Crowley JL, Palmieri SJ, Lifshitz LM, Ehrhardt AG, Hoffman LM, Beckerle MC, Luna EJ. Supervillin modulation of focal adhesions involving trip6/zrp-1. *J Cell Biol*. 2006;174:447-458

36. Fang Z, Takizawa N, Wilson KA, Smith TC, Delprato A, Davidson MW, Lambright DG, Luna EJ. The membrane-associated protein, supervillin, accelerates f-actin-dependent rapid integrin recycling and cell motility. *Traffic*. 2010;11:782-799
37. Modica A, Karlsson F, Mooe T. The impact of platelet function or c-reactive protein, on cardiovascular events after an acute myocardial infarction. *Thromb J*. 2009;7:12
38. Breet NJ, van Werkum JW, Bouman HJ, Kelder JC, Ruven HJ, Bal ET, Deneer VH, Harmsze AM, van der Heyden JA, Rensing BJ, Suttorp MJ, Hackeng CM, ten Berg JM. Comparison of platelet function tests in predicting clinical outcome in patients undergoing coronary stent implantation. *JAMA*. 2010;303:754-762
39. Takafuta T, Wu G, Murphy GF, Shapiro SS. Human beta-filamin is a new protein that interacts with the cytoplasmic tail of glycoprotein ibalpha. *J Biol Chem*. 1998;273:17531-17538
40. Lopez JA, Andrews RK, Afshar-Kharghan V, Berndt MC. Bernard-soulier syndrome. *Blood*. 1998;91:4397-4418
41. Kunishima S, Kamiya T, Saito H. Genetic abnormalities of bernard-soulier syndrome. *Int J Hematol*. 2002;76:319-327
42. Kunishima S, Saito H. Advances in the understanding of myh9 disorders. *Curr Opin Hematol*. 2010;17:405-410
43. Thrasher AJ. New insights into the biology of wiskott-aldrich syndrome (was). *Hematology Am Soc Hematol Educ Program*. 2009:132-138
44. Falati S, Patil S, Gross PL, Stapleton M, Merrill-Skoloff G, Barrett NE, Pixton KL, Weiler H, Cooley B, Newman DK, Newman PJ, Furie BC, Furie B, Gibbins JM. Platelet pecam-1 inhibits thrombus formation in vivo. *Blood*. 2006;107:535-541
45. Signarvic RS, Cierniewska A, Stalker TJ, Fong KP, Chatterjee MS, Hess PR, Ma P, Diamond SL, Neubig RR, Brass LF. Rgs/gi2alpha interactions modulate platelet accumulation and thrombus formation at sites of vascular injury. *Blood*. 2010;116:6092-6100

Figure Legends

Figure 1

GWAS with PFA-100ColA. (A) Manhattan Plots for PFA-100ColA. The Manhattan plot is shown for all autosomes for European and African Americans. The y-axis shows the –log10 of the p-values for the chromosomes numbered on the x-axis. For the African Americans the two most significant SNPs are rs7070678 and rs10826650 in SVIL; both meet genome-wide significance with p-values of $3.6x10^{-8}$ and $4.4x10^{-8}$, respectively. None of the SNPs within *SVIL* meet genome-wide significance for European Americans. (B) *SVIL* region association plot on chromosome 10 for African Americans. The most significant SNP rs7070678 is displayed, and the amount of linkage disequilibrium between this SNP and nearby SNPs is shown as a heat plot with SNPs in strongest LD with rs7070678 in darker colors. The significance level is displayed on the y-axis as –log 10 of the p-values. The rate of recombination within the region is shown as the light blue tracing. The regions containing the *SVIL* and *LYZL1* genes are indicated by green arrows.

Figure 2

SVIL genomic region and transcript expression. (A) Exon structure of SVIL at Chr10:29,786,283-29,963,907 with exons of the two major transcripts (NM_003174, NM_021738) shown as lines and boxes. The location of the 1st of the 5 SNPs (rs7070678) from Table 2 is shown by thin vertical arrows. The locations of the microarray probes are indicated by the thick vertical arrows and ILMN ID numbers. Horizontal arrows indicate the positions of the sense and antisense PCR primers. (B) Ethidium-stained agarose gel showing RT-PCR products of leukocyte-depleted platelet (LDP) RNA and primers specific for ITGA2 (CD41, integrin αIIb) and SVIL. Neg, no template control. (C) Box plot showing the levels of

SVIL mRNA (ILMN_1671404) in LDP (n=29), PRP (n=11) and CD45+-leukocytes (WBC; n=5). Box represents interquartile range and whiskers represent 5% - 95% range.

Figure 3

Platelet supervillin expression. (A) Immunoblot of PRP and, as a positive control, the A549 human alveolar adenocarcinoma cell line. Blots were probed with anti-supervillin (SVIL) and anti-CD41 (platelet integrin αIIb) antisera and imaged on a LI-COR Odyssey. GAPDH, loading control. (B) Supervillin protein schematic showing locations of the gelsolin/villin homology repeats, the binding sites for myosin II heavy chain (Myo II) and F-actin, and the epitopes for the 4 antibodies used (H340, Ab50856, HPA02013 and S8695). (C) Immunoblot probed with anti-SVIL antibody S8695 and anti-CD45. The erythroleukemia K562 and megakaryocytic Meg-01 cell lines are included. (D) Immunoblot with additional anti-SVIL antibodies. (E) Immunoblot with H340 using lysates from mouse platelets and from A549 and HeLa adenocarcinoma cells, as controls.

Figure 4

Correlation of *SVIL* mRNA levels with human platelet function. Natural log transformed *SVIL* mRNA levels (VSTs) from the gene expression profiling were correlated with (**A**) PFA-100ColA closure times, (**B**) mean platelet volume (MPV) and (**C**) *SVIL* expression levels based on rs7070678 genotype.

Figure 5

Disruption of the *Svil* gene and loss of Svil expression in platelets. (**A**) Diagram of the wild-type (WT) and mutated (Mut) *Svil* loci (top 2 lines) with enlargements (bottom 2 lines) showing the insertion site (*****) of the pGT0lxf vector sequence within the intron between coding exons 13 (E-13) and 14 (E-14). Also shown are the locations of PCR primer sets diagnostic for the wild-type

and mutant loci (arrows), the 0.8-kb probe used for Southern analyses, and the Bgl II sites (triangles) associated with endogenous genomic DNA and with the inserted β-galactosidase-neomycin (β-gal/neo) coding sequence. (**B**) PCR of genomic DNA from mouse tails using the primer sets shown in Panel A. Primers specific for the insertion identify a ~2.5-kb product (Mut, top) while primers specific for the wild-type allele generate a 0.8-kb product (WT, below). (**C**) Immunoblot of mouse platelets with anti-supervillin antibody (H340) and anti-tubulin as a loading control.

Figure 6

Enhanced adhesion and thrombus formation in platelets lacking supervillin. Whole blood from wild type (WT, black line) or *Svil-/-* (SVIL, red line) mice was perfused over immobilized collagen at venous (400 s^{-1}) or arterial (1200 s^{-1}) shear conditions. Platelets in whole blood were labeled with AlexaFluor488-labeled antibodies to platelet GPIX before perfusion. (**A, C**) Surface area covered by platelets at indicated time points presented as % of coated collagen ± SEM. (**B, D**) Sum fluorescence intensity ± SEM measured at the indicated time points. Experiments shown in panels A-D were conducted on 4 different days for a total of 15 runs for each genotype. (**E**) Representative images were taken at the designated times during perfusion at arterial (1200 s^{-1}) shear rates. Scale bars shown in 1-min images apply to all time points.

Figure 7

Immunofluorescence micrographs of (**A, B, E, F**) wild-type or (**C, D, G, H**) supervillin-deficient platelets fixed (**A-D**) statically onto glass or (**E-H**) after activation for 2 min on collagen under high-shear (1200 s^{-1}) flow. F-actin (*red*) was visualized with AlexaFluor568-phalloidin; myosin IIA (*green*) was stained with antibody. Bars, 2.5 μm, 0.5 μm, and 12.5 μm, as indicated.

Table 1. Demographics of subjects in this genetic study.

Parameters	**African American**	**European Americans**
No. of Subjects	116	125
Females	69%	50%
Mean Age (yrs) ± SD	35.0 ± 9.4	35.0 ± 11.1
Mean BMI (kg/m^2) ± SD	28.6 ± 5.3	25.5 ± 4.6
Smokers	16.4%	32%
Hypertension	8.6%	3.4%
Hematocrit (%) ± SD	36.1 ± 5.0	37.4 ± 4.4
Fibrinogen (mg/dL) ± SD	345 ± 99	300 ± 64
VWF activity (%) ± SD	88 ± 38	79.7 ± 35
PRP platelet count (per µL) ± SD	406,060 ± 93,350	430,550 ± 111,600

Table 2. Most significant p-values detected in genotype data from African Americans

SNP ID	Chr:position	Genes	β	Std Error	MAF*	Type	P value
rs7070678	10:29812602	SVIL	-0.006807	0.001235	.327	Exon 14 synonymous	3.581×10^{-8}
rs10826650	10:29814284	SVIL	-0.006856	0.001253	.340	Intron 13	4.426×10^{-8}
rs11858159	15:24824188	PWRN1	0.005737	0.001169	.366	Intron 7	9.1879×10^{-7}
rs3901472	15:24814582	PWRN1	0.005773	0.001182	.379	Intron 3	1.034×10^{-6}
rs7656730	4:40159617	N4BP2	0.025637	0.005250	.675	3' UTR	1.044×10^{-6}
rs7910521	10:29803661	SVIL	-0.006104	0.001279	.326	Intron 16	1.830×10^{-6}
rs10826649	10:29792539	SVIL	-0.006142	0.001301	.297	Intron 17	2.382×10^{-6}
rs17783459	18:42329076	SETBP1	0.032067	0.006898	.042	Intron 3	3.343×10^{-6}
rs9890514	17:46738883	none	0.012391	0.002675	.196	-	3.604×10^{-6}
rs1507740	1:163075021	none	0.013215	0.002885	.157	-	4.640×10^{-6}

***** Minor allele frequency

Table 3. Platelet parameters in wild type and *Svil -/-* mice.

Parameter	**wild type**	***Svil -/-***	**P value***
Platelet number/μL†	1,083,000	969,000	0.67
Forward scatter‡	19.4	23.2	<0.0001
Surface area (μm^2)§	4.7 ± 0.1 (N=159)	5.3 ± 0.1 (N=241)	0.0045
Integrin αIIb , MFI ‖ fold change#	1.02		0.89 (n.s.)
GPIbα, MFI ‖ fold change#	1.30		0.40 (n.s.)

* Calculated by Student's T-Test

† By Hemavet 850FS (Drew Scientific)

‡ By FACScan (Becton Dickinson)

§ Means ± s.e.m. by confocal microscopy of AlexaFluor568-phalloidin stained unactivated

‖ MFI, mean fluorescence intensity ratio of mutant/wild type platelets

Flow cytometric comparisons between mice are shown as fold-changes to normalize for day-to-day variation in platelets, antibody fluorescence, binding, and acquisition.

A

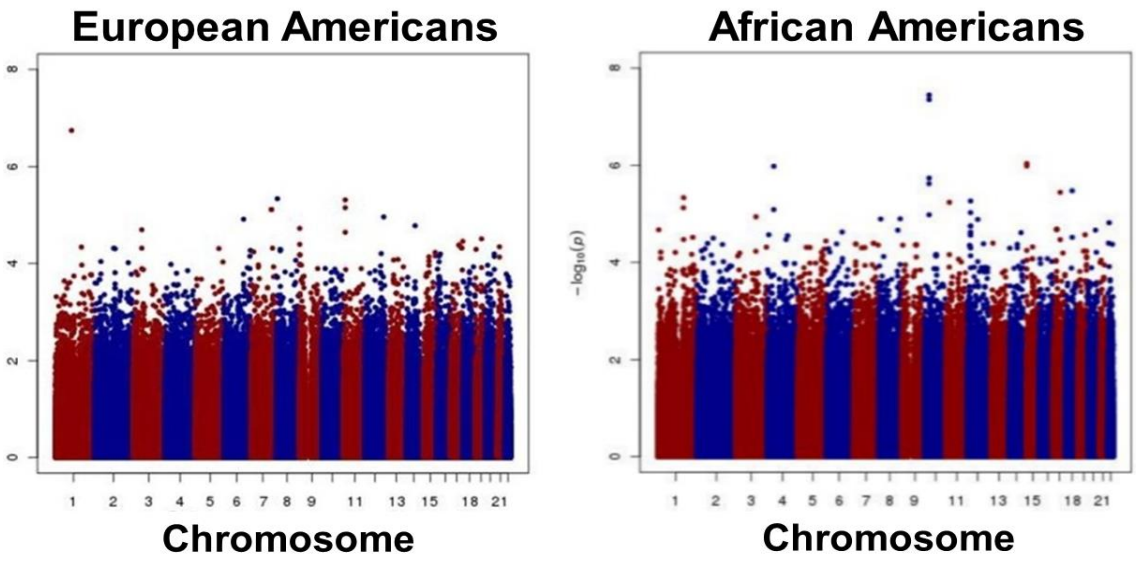
European Americans
African Americans
Chromosome
Chromosome

B

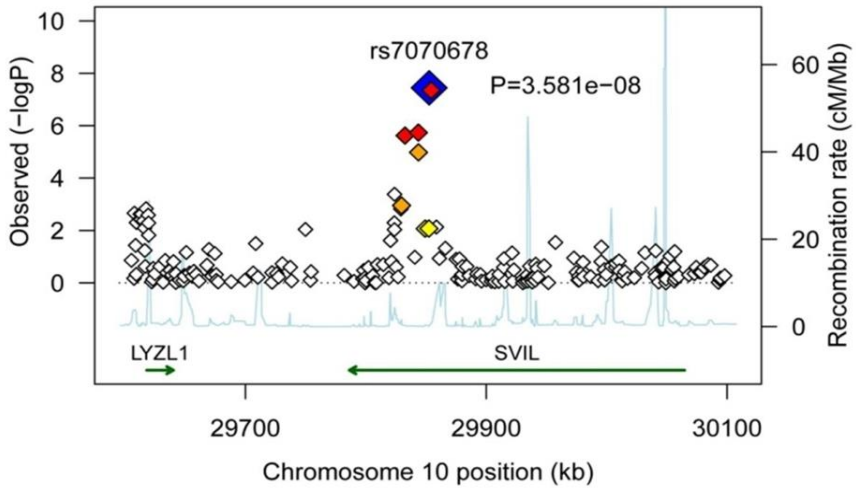
rs7070678
P=3.581e−08
Observed (−logP)
Recombination rate (cM/Mb)
LYZL1
SVIL
29700
29900
30100
Chromosome 10 position (kb)

Figure 1

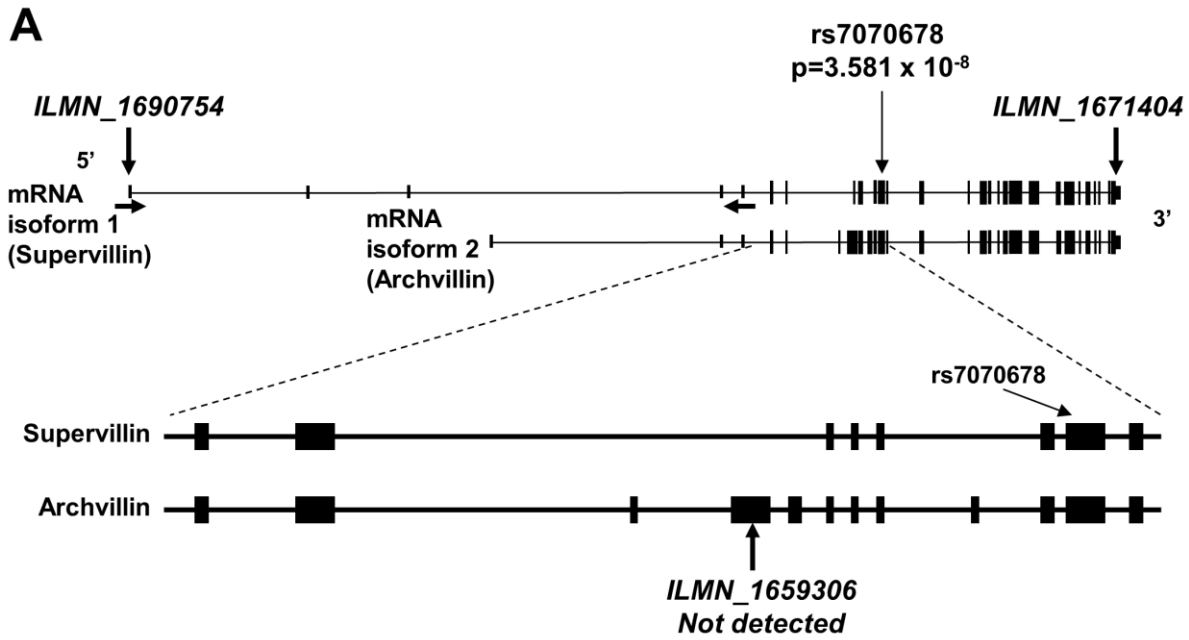
A
rs7070678
p=3.581 x 10-8
ILMN_1690754
ILMN_1671404
5'
3'
mRNA
isoform 1
(Supervillin)
mRNA
isoform 2
(Archvillin)
rs7070678
Supervillin
Archvillin
ILMN_1659306
Not detected

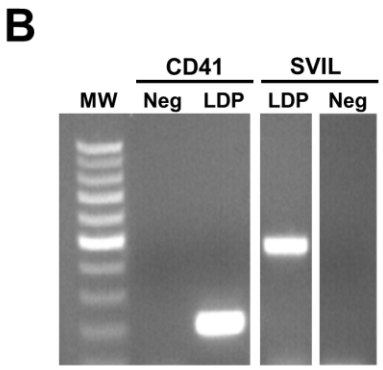
B
CD41
SVIL
MW
Neg
LDP
LDP
Neg

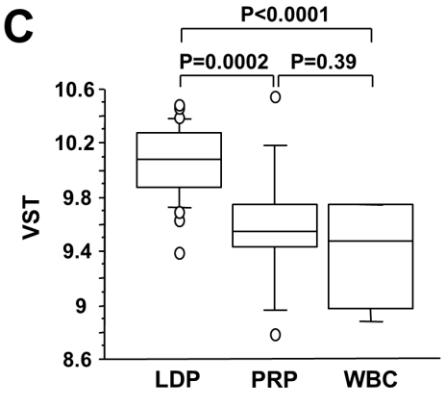
C
P<0.0001
P=0.0002
P=0.39
10.6
10.2
9.8
9.4
9
8.6
VST
LDP
PRP
WBC

Figure 2

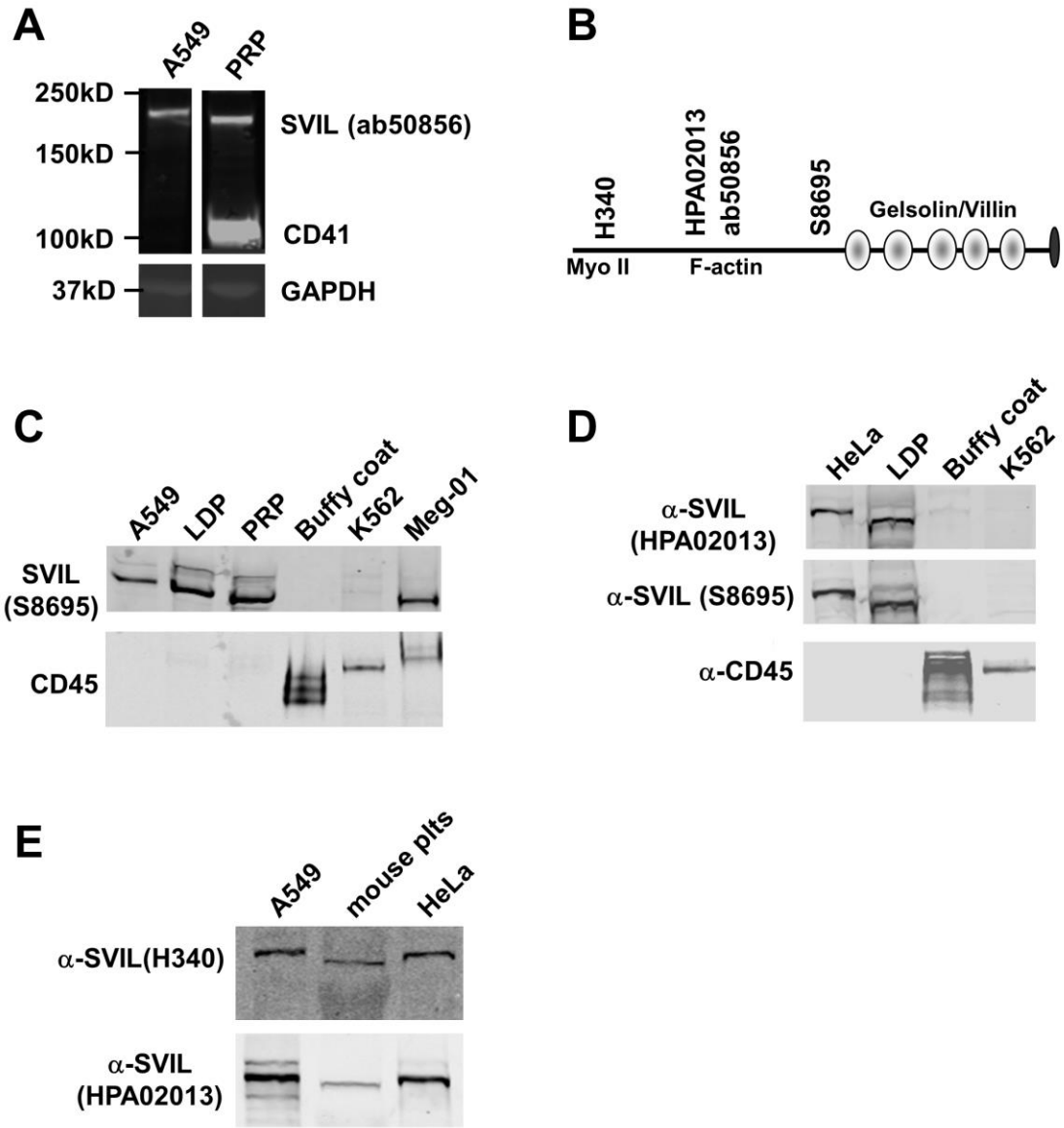
A
A549
PRP
250kD
150kD
100kD
37kD
SVIL (ab50856)
CD41
GAPDH
B
H340
HPA02013
ab50856
S8695
Gelsolin/Villin
Myo II
F-actin
C
A549
LDP
PRP
Buffy coat
K562
Meg-01
SVIL
(S8695)
CD45
D
HeLa
LDP
Buffy coat
K562
α-SVIL
(HPA02013)
α-SVIL (S8695)
α-CD45
E
A549
mouse plts
HeLa
α-SVIL(H340)
α-SVIL
(HPA02013)

Figure 3

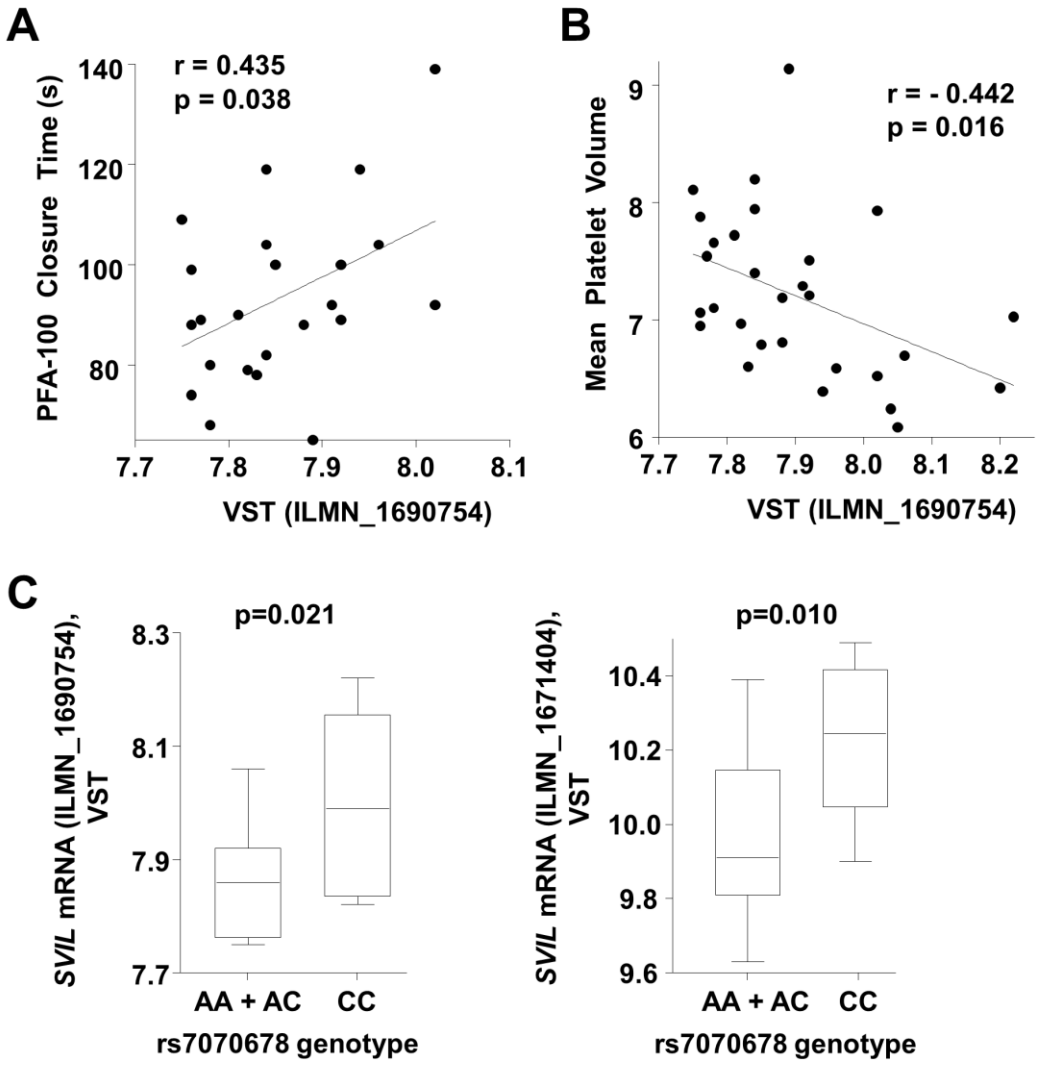
A
PFA-100 Closure Time (s)
r = 0.435
p = 0.038
VST (ILMN_1690754)
B
Mean Platelet Volume
r = - 0.442
p = 0.016
VST (ILMN_1690754)
C
SVIL mRNA (ILMN_1690754), VST
p=0.021
AA + AC
CC
rs7070678 genotype
SVIL mRNA (ILMN_1671404), VST
p=0.010
AA + AC
CC
rs7070678 genotype

Figure 4

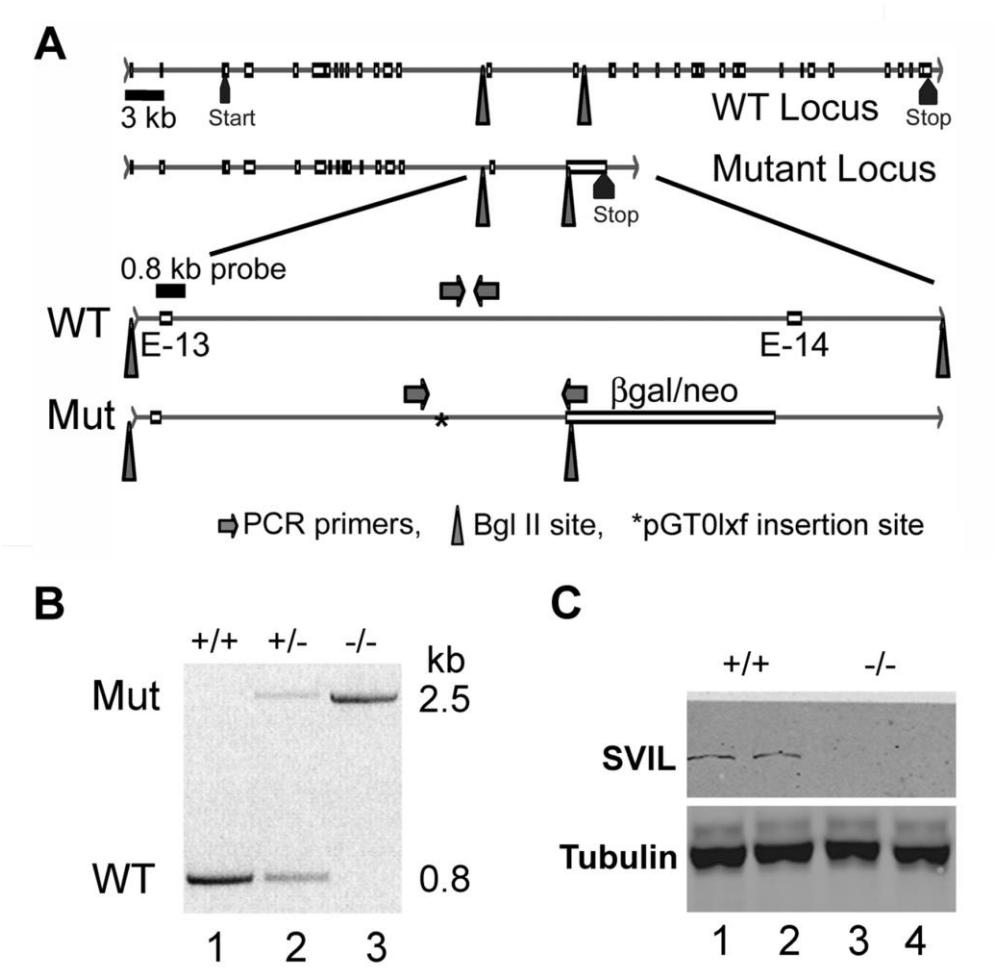
A
3 kb
Start
WT Locus
Stop
Mutant Locus
Stop
0.8 kb probe
WT
E-13
E-14
Mut
βgal/neo
PCR primers,
Bgl II site,
*pGT0lxf insertion site
B
+/+
+/-
-/-
kb
Mut
2.5
WT
0.8
1
2
3
C
+/+
-/-
SVIL
Tubulin
1
2
3
4

Figure 5

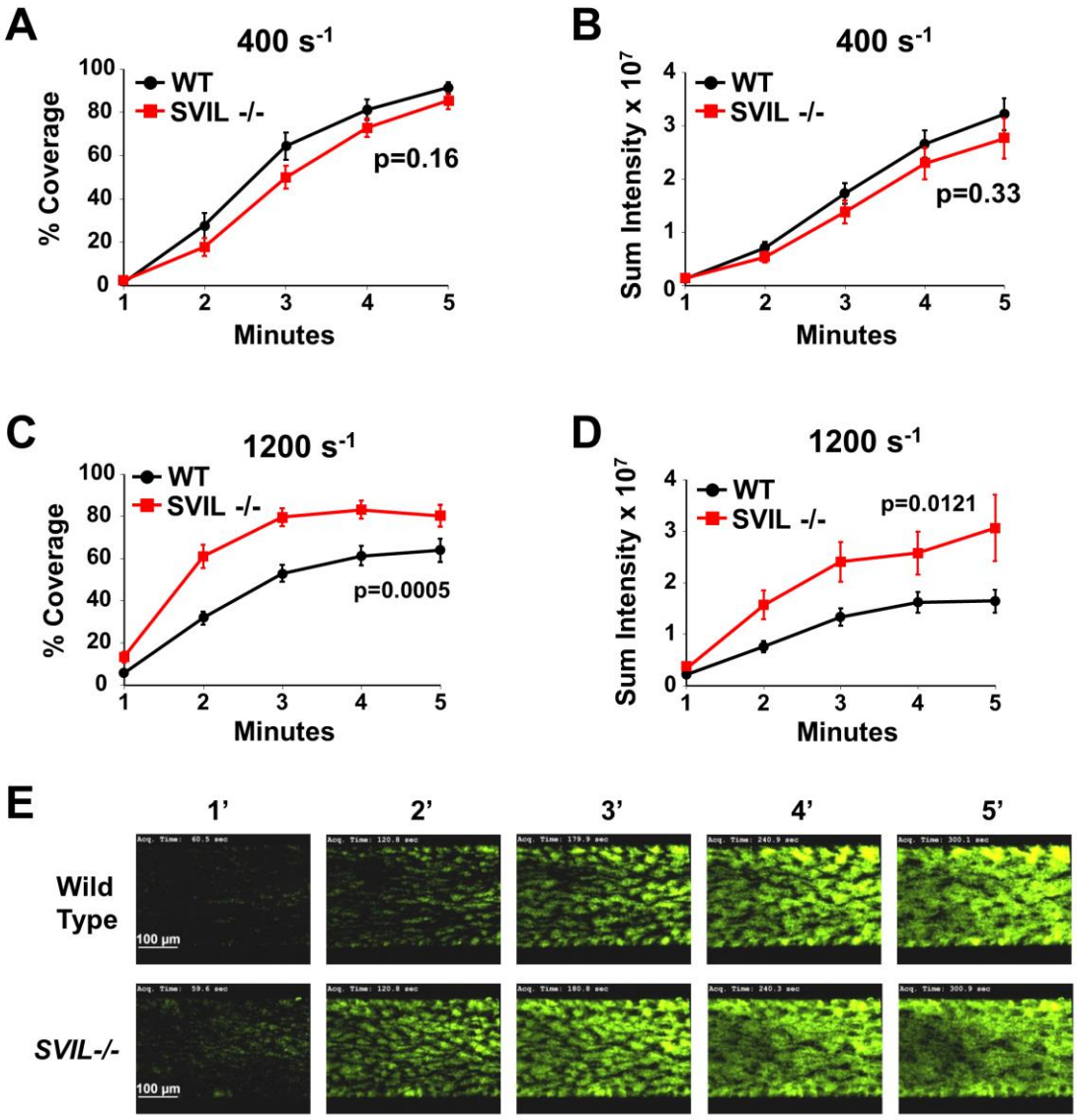
A
400 s-1
WT
SVIL -/-
p=0.16
% Coverage
Minutes
B
400 s-1
WT
SVIL -/-
p=0.33
Sum Intensity x 10^7
Minutes
C
1200 s-1
WT
SVIL -/-
p=0.0005
% Coverage
Minutes
D
1200 s-1
WT
SVIL -/-
p=0.0121
Sum Intensity x 10^7
Minutes
E
1'
2'
3'
4'
5'
Wild Type
SVIL-/-
100 µm
100 µm

Figure 6

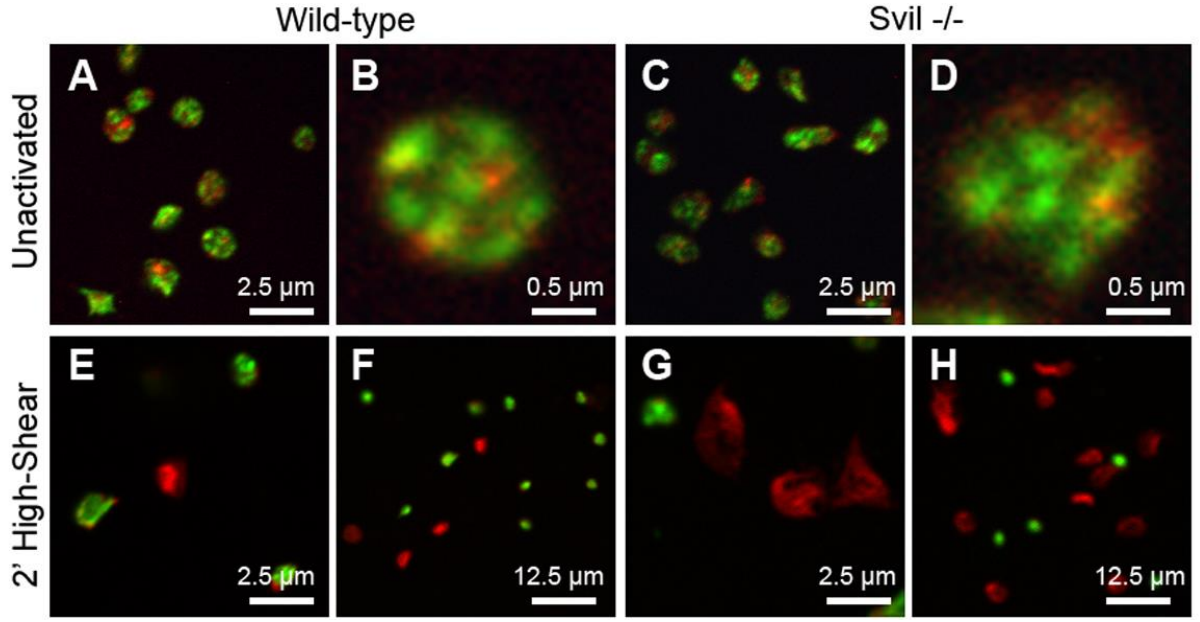
Wild-type
Svil -/-
Unactivated
2' High-Shear
A
B
C
D
E
F
G
H
2.5 µm
0.5 µm
2.5 µm
0.5 µm
2.5 µm
12.5 µm
2.5 µm
12.5 µm

Figure 7